Optical resolution below λ/4 using synthetic aperture microscopy and evanescent-wave illumination

Alexander Neumann,* Yuliya Kuznetsova, and S. R. J. Brueck

Center for High Technology Materials and Departments of Physics and Astronomy and Electrical and Computer Engineering, University of New Mexico, 1313 Goddard SE, Albuquerque, New Mexico, USA
**Corresponding author: aneumann@chtm.unm.edu*

Abstract: Evanescent-wave illumination is applied to synthetic-aperture microscopy on a transparent solid substrate to extend the resolution limit to $\lambda/2(n+1)$ (where n is the substrate refractive index) independent of the lens NA. Using a 633 nm source and a 0.4 NA lens, a resolution to 150 nm ($\lambda/4.2$) is demonstrated on a glass ($n = 1.5$) substrate. Further extension to ~ 74-nm resolution ($\lambda/8.6$) is projected with a higher index substrate ($n = 3.3$).

©2008 Optical Society of America

OCIS codes: (190.0190) Microscopy; (110.3175) Interferometric imaging.

References and links

1. E. Abbé, "Beiträge zur Theorie des Mikroskops und der Mikroskopischen Wahrnehmung," Arch. Mikrosc. Anat. Entwicklungsmech. **9**, 413–468 (1873).
2. W. Lucosz, "Optical Systems with Resolving Powers Exceeding the Classical Limit," J. Opt. Soc. Am. **57**, 932-941 (1967).
3. H. Nassenstein, "Superresolution by diffraction of subwaves", Opt. Commun. **2**, 231-234 (1970).
4. C. J. Schwarz, Y. Kuznetsova, and S. R. J. Brueck, "Imaging interferometric microscopy," Opt. Lett. **28** 1424-1426 (2003).
5. Y. Kuznetsova, A. Neumann, and S. R. J. Brueck, "Imaging interferometric microscopy – approaching the linear systems limits of optical resolution," Opt. Express **15**, 6651-6663 (2007).
6. S. A. Alexandrov T. R. Hillman, T. Gutzler, and D. D. Sampson, "Synthetic aperture Fourier holographic optical microscopy," Phys. Rev. Lett. **97** 168102 (2006).
7. V. Mico, Z. Zalevsky, and J. Garcia, "Superresolution optical system by common-path interferometry," Opt. Exp. **14,** 5168-5177 (2006), http://www.opticsinfobase.org/abstract.cfm?URI=oe-14-12-5168.
8. Y. Kuznetsova, A. Neumann, and S. R. J. Brueck, "Imaging interferometric microscopy," J. Opt. Soc. Am. **A 25**, 811-822 (2008).
9. A. Neumann, Y. Kusnetsova, and S. R. J. Brueck, "Structured Illumination for the Extension of Imaging Interferometric Lithography," Opt. Express **16**, 6785-6793 (2008).
10. D. Axelrod, "Total Internal Reflection Fluorescence Microscopy in Cell Biology," Traffic, **2**, 764-774 (2001).
11. G. E. Cragg and P. T. C. So, "Lateral resolution enhancement with standing evanescent waves," Opt. Lett. **25**, 46-48 (2000).
12. S .W. Hell, "Far-Field Optical Nanoscopy," Science **316**, 1153-1158 (2007).
13. A. Vainrub, O. Pustovyy, and V. Vodyanoy, "Resolution of 90 nm (λ/5) in an optical transmission microscope with an annular condenser," Opt. Lett. **31**, 2855-2857 (2006).
14. Q. Wu, L. P. Ghislan, and V. B. Elings, "Imaging with Solid Immersion Lenses, Spatial Resolution, and Applications," Proc. IEEE **88**, 1491-1498 (2000).
15. J. Pendry, "Negative Refraction Makes a Perfect Lens," Phys. Rev. Lett. **85**, 3966-3969 (2000).
16. V. Podolskiy and E. E. Narimanov, "Near-Sighted Superlens," Opt. Lett. **30**, 75-77 (2005).
17. Z. Liu, H. Lee, Y. Xiong, C. Sun, and X. Zhang, "Far-Field Optical Hyperlens Magnifying Sub-Diffraction-Limited Objects," Science **315**, 1686 (2007).
18. H. Lee, Z. Liu, Y. Xiong, C. Sun, and X. Zhang, "Development Of Optical Hyperlens for Imaging Below the Diffraction Limit," Opt. Express **15**, 15886-15891 (2007).
19. I. I. Smolyaninov, Y-J. Hung, and C. C. Davis, "Magnifying Superlens in the Visible Frequency Range," Science **315**, 1699-1701 (2007).

#102125 - $15.00 USD Received 29 Sep 2008; revised 11 Nov 2008; accepted 14 Nov 2008; published 25 Nov 2008

20. D. F. Nelson and E. H. Turner, "Electro-optic and Piezoelectric Coefficients and Refractive Index of Gallium Phosphide," J. Appl. Phys. **39**, 3337-3343 (1968).

1. Introduction

Improvement of optical microscopy resolution is an age-old quest. The classical resolution limits, first described by Abbé [1], are a pitch of λ/NA and a corresponding resolution of $\lambda/2NA$ for normal incidence coherent illumination where NA is the objective lens numerical aperture. This corresponds to the largest tilt of a diffracted order that is transmitted through the lens. For off-axis coherent illumination, this limit is extended to $\lambda/4NA$, corresponding to illumination and collection of diffracted information on opposite edges of the lens focal plane aperture (of diameter $2NA$). In previous work [2-9], we and others have shown that this limit can be extended to $\lambda/4$, independent of the lens NA using a synthetic aperture approach to effectively increase the illumination and collection *NA*s to 1 in a piecewise fashion. Recently, we have demonstrated [4,9] resolution of complex patterns almost to these linear systems limits, ~ $\lambda/3.5$ ~ 180 nm at a 633 nm wavelength, by imaging interferometric microscopy (IIM), consisting of dark-field illumination along with interferometric reintroduction of a zero-order reference beam at the square-law detection plane. Here, we combine this synthetic aperture approach with evanescent-wave illumination to extend the frequency space coverage to $\lambda/(n+1)$ [resolution to $\lambda/2(n+1)$] and demonstrate a large field (~ 10×10 μm^2) resolution to ~ 150 nm ($\lambda/4.2$) with a glass substrate (refractive index, $n_{sub} = 1.51$) at a 633-nm wavelength.

Total-internal-reflection fluorescence (TIRF) microscopy uses a similar illumination configuration; however TIRF resolution is limited by the NA of the collection lens as described above. The major advantage of TIRF, the restriction of the excitation volume to within an evanescent field decay length of the high-index substrate, has been applied extensively for surface studies [10] providing ~ 10× enhancement of the axial resolution. A lateral resolution enhancement for fluorescence microscopy was achieved with standing evanescent wave illumination [11]. Nonlinear fluorescence microscopy techniques have been demonstrated to enhance the resolution well beyond these linear systems limits (for a recent review see Ref. 12) The nonlinear response extends the spatial frequency coverage and allows impressive results, however these techniques typically require specific fluorophores and complex laser source/optical systems and often require point-by-point scanning. There remains a need to extend linear (transmission/reflection) microscopy to smaller scales. While our IIM approach is not directly extendable to fluorescence microscopy as a result of the lack of coherence between the excitation and emission wavelengths, extension to a coherent anti-Stokes Raman (CARS) configuration allows chemical specificity along with enhanced resolution.

Immersion techniques to extend the frequency space coverage of microscopy [to NA~1.4 to 1.6; *i.e.* ~$\lambda/6$] are well established [13], but remain limited in application as a result of practical issues such as compatibility of immersion fluids with the sample or the difficulties of assuring close approach (within fractions of a wavelength) of a solid immersion lens [14]. Additionally, the full potential of immersion (up to refractive indices of ~3.5) has not been realized as a result of the difficulties of producing aberration-corrected lenses at these high *NA*s along with the absence of appropriate index-matching fluids.

Near-field optical probes (NSOM) offer another approach to extending the resolution that is complicated by the same mechanical difficulties, by the electromagnetic interaction of the probe with the sample, by the small signal levels associated with coupling to the subwavelength tip, and by a slow point-by-point modality. NSOM is often combined with evanescent wave illumination.

Much of the scientific excitement associated with metamaterials has been driven by the possibility of "perfect lenses" that operate without any transverse spatial-frequency bandpass limitation [15]. This improved resolution is necessarily restricted to near-field domains for flat lenses and remains limited by materials, fabrication and impedance-matching constraints [16]. Related hyperlenses, which take advantage of nonplanar metamaterial/plasmonic variations to generate magnification, convert the evanescent fields at the object to propagating fields at the

#102125 - $15.00 USD Received 29 Sep 2008; revised 11 Nov 2008; accepted 14 Nov 2008; published 25 Nov 2008
(C) 2008 OSA

image and have demonstrated resolution to ~ λ/3 [17,18] and to λ/7 [19]. The geometric constraints associated with the hyperlens severely restrict the field-of-view, to date to only a few times the resolution. In the case of a 2D, planar, hyperlens structure [19] the image is necessarily restricted to a 1D line image.

2. Resolution improvement with evanescent-wave illumination

This contribution reports an extension of IIM to evanescent illumination from a high-index substrate, effectively half (solid) immersion IIM. The interferometric reintroduction of a zero-order beam allows unambiguous capture and retrieval of the information corresponding to the propagating diffracted waves scattered by the object from the evanescent-wave illumination. This expands the frequency space coverage of IIM to a circle of radius $NA_{eff} \leq (n_{sub} + 1)$, where n_{sub} is the refractive index of the substrate. In these initial experiments, the substrate was glass with $n_{sub} \sim 1.51$ giving $NA_{eff} \leq 2.51$ [2.32 achieved experimentally; half-pitch resolution λ/4.64]. An interferometric introduction of the zero-order diffracted beam (reflection or transmission as appropriate) in the back Fourier plane of the objective completes the optical scheme. Extension to higher-index materials is straightforward and will provide extensive further resolution enhancement. For example, GaP has an index of 3.3 at 633 nm [20], and the spatial bandwidth therefore extends to $NA_{eff} \leq 4.3$ (half-pitch resolution to λ/8.6). In contrast to probe-based NSOM approaches, the IIM arrangement does not require close approach of a probe tip to the sample as the object scatters the evanescent illumination, coupled through the substrate, into propagating diffracted waves that are collected in a standard, full-field microscope configuration.

The IIM optical arrangement[4] with an extreme off-axis (dark-field) illumination beam and a coherent reference beam, reinjected into the objective lens Fourier plane using an optical fiber, is illustrated in Fig. 1(a). Here, instead of off-axis illumination in air (Fig. 1(b)) we use illumination propagating beyond the total-internal reflection (TIR) angle in the transparent substrate in the same set up (Fig. 1(c)). The evanescent wave associated with the TIR extends beyond the substrate into the sample region where it is scattered by the subwavelength sample structure into propagating waves that provide information on the details of the object at spatial frequencies up to $(n_{sub}+NA)/\lambda$ (Fig. 1(c)) and $(n_{sub}+1)/\lambda$ with a tilted optical axis (Fig. 1(d)). The object spatial information is contained in the amplitude and phase of the scattered fields at wavevectors corresponding to the difference between the illumination and collection wavevectors. Hyperlenses concentrate on collection of higher spatial frequency (evanescent) information in the scattered field with conventional illumination; here we emphasize evanescent illumination and collection of propagating, far-field scattered fields.

The tilted optical system, Fig. 1(d), is manifestly non-paraxial and the spatial frequencies measured in the laboratory frame have to be corrected before assembling a final composite image. This procedure has been described in detail previously [4,7] and is not reiterated here. The frequency rescaling procedure also restores the field of view that is limited in the laboratory frame by the depth-of-field of the microscope objective optical system. To ease the

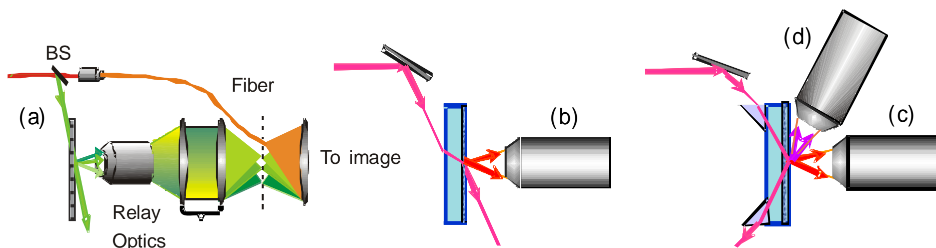

Fig. 1. Optical arrangements for IIM. a) IIM with a zero-order reference beam interferometrically reinjected in the back-pupil plane. b) Expanded view of illumination and detection configuration; c) Illumination through substrate to enhance the spatial frequency coverage; d) Rotated optical axis to collect higher spatial frequency information

#102125 - $15.00 USD Received 29 Sep 2008; revised 11 Nov 2008; accepted 14 Nov 2008; published 25 Nov 2008
(C) 2008 OSA

requirements on the camera pixel size and count, it is possible to offset the angle of the zero-order reference to reduce the measured spatial frequencies and then computationally restore the high spatial frequencies of the object in post-processing [9].

The resolution limit now depends on the refractive index of the substrate. For a glass substrate with $n_{sub} = 1.51$ and an $NA = 0.4$ objective, the $NA_{eff} \le 1.91$ (geometry of Fig. 1(c)), allowing resolution of 166-nm half-pitch grating structures with $\lambda = 633$ nm. NA_{eff} is extended to ≤ 2.51 for the tilted optical-axis geometry of Fig. 1(d) with a corresponding minimum half-pitch to 126 nm. These resolution limits apply to simple grating structures (which have narrow Fourier spectra), for more complex structures such as the test pattern experimentally demonstrated, the pattern-dependent resolution is somewhat lower as a result of the need to capture additional information in the sidebands around the main diffraction peaks.

A Manhattan (*x*-,*y*-geometry) test pattern is shown in Fig 2(a). This pattern is scaled to different dimensions for the present experiments. The Fourier intensity transform of this pattern for a linewidth (critical dimension or CD) of 180 nm is shown in Fig. 2(b) and for a CD of 150 nm in Fig. 2(c). The circles in Figs. 2(b) and 2(c) correspond to the bandpass limits of various microscopy configurations. The circle in the center of Fig. 2(b), with a radius of $NA/\lambda = 0.4/\lambda$, corresponds to the Abbé-limit spatial frequency range captured with on-axis coherent illumination ($NA_{ill} = 0$). The inner set of shifted circles in Fig. 2(b) (only single sidebands are shown for clarity; the complex conjugate regions are covered as well) correspond to IIM with off-axis illumination beams at $\alpha_{ill} = 53°$ in the *x*-, *y*-directions that extend the frequency coverage to a radius $3NA/\lambda \sim 1.2/\lambda$. Additional frequency space coverage (second pair of circles) is available using evanescent wave illumination extending the frequency space coverage to a radius of $(n_{sub} sin\alpha_{ill}+NA)/\lambda \sim 1.87/\lambda$ (with $\alpha_{ill} = 76°$) without tilt of the microscope optical axis. We have previously reported a similar frequency space coverage and resolution using tilt of the optical axis (Fig. 1(d)) and illumination at grazing incidence in air [4,7].

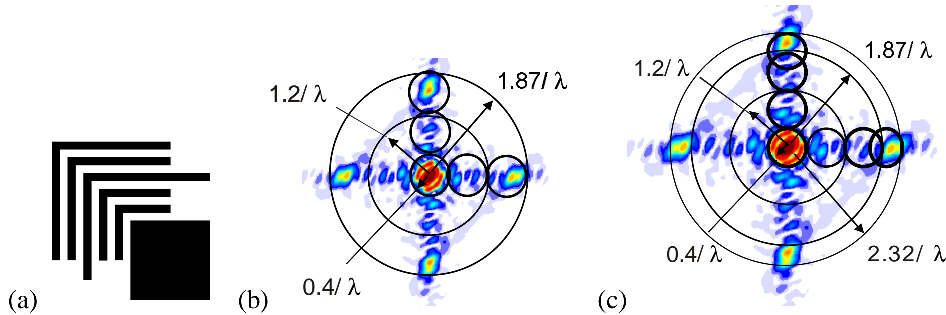

Fig. 2. Frequency-space visualization of IIM. a) Manhattan structure test pattern; scaled to different sizes as indicated; b) frequency space coverage for the structure with CD = 180 nm which is resolved for the configuration of Fig. 1(b); c) frequency space coverage for the structure with CD = 150 nm which requires the optical axis tilted configuration of Figure 1(c).

The experimental result for an object containing both 180- and 170- nm CD structures in a single large-field image is shown in Fig. 3(a). The 180-nm CD object is within the bandwidth capabilities of this optical system while the 170-nm CD object has significant spatial frequencies that extend beyond the optical system bandwidth and so is not fully resolved. The five nested "ell" shapes are distinguishable for the 180-nm CD, but not for the 170- nm CD. The positions of the two objects are correctly restored by the image restoration procedure as is evident from the good positional overlap between the experimental and theoretical cross-cuts in Fig. 3(b).

#102125 - $15.00 USD Received 29 Sep 2008; revised 11 Nov 2008; accepted 14 Nov 2008; published 25 Nov 2008
(C) 2008 OSA

Including tilt of the optical axis, additional spatial frequencies are accessible and the resolution becomes independent of *NA*. Ideally, we should be able to resolve 126-nm grating

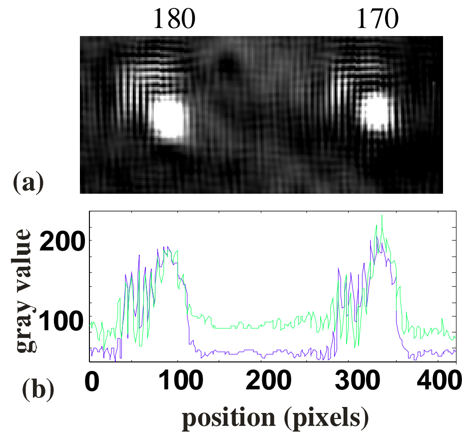

Fig. 3. IIM with evanescent illumination and normal (untilted) collection. a) Reconstructed image of 180- and 170-nm CD structures b) a crosscut (green) compared with a crosscut of corresponding simulation (blue).

structures using a n_{sub} =1.51 glass substrate and a tilt angle of $\theta = 90° - \sin^{-1}(NA) = 66°$. Experimentally, we used an illumination angle (in the glass), α_{ill}, of 76° and a tilt angle of 35° and achieved $N_{eff} = n_{sub}\sin(a_{ill}) + \sin\left(\theta + \sin^{-1} NA\right)$ ~ 2.32 (which allows 137 nm half-pitch grating resolution) and resolution of patterns with 150-nm CD features which is beyond the half-pitch linear systems limit in air of λ/4 ~ 158 nm, clearly demonstrating the evanescent coupling. The frequency space coverage along with the corresponding structure Fourier intensity plot is shown in Fig. 2(c). The third pair of off-axis sub-images in Fig. 2(c) correspond to the tilted optical axis. This frequency region is elliptical rather than circular, due to nonparaxial and conical diffraction effects associated with the of-axis optical system [4,7].

In order to decrease the influence of the camera pixel discretization on this high frequency image, the reference beam was adjusted to provide lower intermediate frequencies on the imaging camera which were reconstructed computationally [9]. The final result is shown in Fig. 4(a) along with the corresponding model, Fig. 4(b), and the crosscut comparison in Fig. 4(c). Very good agreement is achieved.

The overall quality of the image (even in the model) is not as well-defined as for the 180-nm image. Inspection of Figs. 2(b) and 2(c) shows the reason. Scaling of the frequency space coverage to get an equivalent image resolution requires both: increasing the high frequency coverage along the principal axes, which we have accomplished; and additional coverage away from the principal axes, which we have yet to add. For the smaller pattern, the frequency content spreads away from the major axes and less of the important frequency information is captured in the present configuration. Additionally, Gibb's effects resulting from the hard cutoff in frequency response in a region with strong spectral content, and the required precision in setting and measuring the tilt and illumination angles make it more difficult to obtain high-quality, extended-field images as the frequency coverage is increased. The noise of the system causes problems for combination of the image from seven (or more) sub-images. We will address these problems in future work.

IIM is a spatial wavelength-division-multiplex approach to optical microscopy that approaches ultimate linear systems (diffraction) limits for microscopy, using only low numerical aperture objective lenses and retaining the depth-of-field, field-of-view and

#102125 - $15.00 USD Received 29 Sep 2008; revised 11 Nov 2008; accepted 14 Nov 2008; published 25 Nov 2008
(C) 2008 OSA

working-distance advantages of the low numerical aperture system. In this paper we demonstrate further resolution improvement by using evanescent wave illumination. Experimental results with resolution of complex objects to λ/3.72 without tilt of the optical axis and to λ/4.22 with tilt of the axis have been presented.

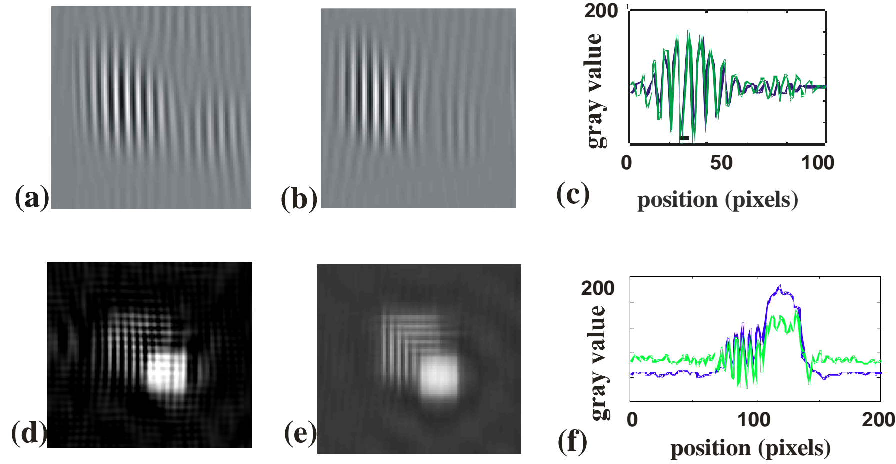

Fig. 4. IIM of a 150 nm structure using evanescent illumination and a tilted optical system. a) High-frequency image obtained by evanescent wave illumination and tilted optical system; b) high-frequency image simulation and experiment; c) experimental and simulation cross-cuts of the high-frequency sub-images; d) experimental composite (full) image; e) simulation full image; f) experimental and simulation cross-cuts of the full images.

Evanescent illumination can be combined with structural illumination eliminating the need for access to the back focal plane [9]. This moves the interferometer to the front of the objective lens and makes IIM readily adaptable to existing microscopes. Structural illumination is roughly equivalent to recording the spectral information at an intermediate frequency; additional computation is required to reset the frequencies. As noted, we have already taken advantage of this frequency shifting to reduce the camera pixel size and count requirements.

3. Conclusions

Evanescent wave illumination has been used to extend the resolution of IIM to λ/2(*n*+1). Images of 150-nm structures (arbitrary Manhattan geometry pattern) using a 633 nm wavelength (λ/4.2) demonstrates optical resolution below λ/4, the linear systems limit of available resolution in air. Further resolution improvement with this half-immersion geometry is available for a substrate with a higher refractive index (GaP with $n = 3.3$ allows NA_{eff} of 4.3 and a corresponding periodic pattern half-pitch resolution of 74 nm = λ/8.6 at 633 nm). The conceptually straightforward full immersion extension will further increase the NA_{eff} to $2n$ (= 6.6 for GaP) and the corresponding half-pitch resolution to 48 nm (λ/13). In this context, it is worthwhile to note that IIM provides an important advantage over conventional immersion microscopy techniques. Since only a relatively small region of frequency space (~ *NA/λ)* is recorded in each sub-image, the aberration requirements on the objective lens are dramatically reduced. We envision using a simple set of prisms or gratings to extract, and conventional air-based lenses to capture, the information. As is always the case, there is a trade-off between the number of sub-images and the *NA* of the objective lens.

#102125 - $15.00 USD Received 29 Sep 2008; revised 11 Nov 2008; accepted 14 Nov 2008; published 25 Nov 2008
(C) 2008 OSA

The possible increase of NA_{eff} is shown in Fig. 5, drawn for a 0.4 *NA* system. As the frequency coverage is extended, the use of higher *NA* lenses will reduce the number of sub-images required for a more complete coverage of frequency space. Of course the required coverage is dependent on the pattern, and there are some applications, for example in metrology for integrated circuits, where coverage of a subset of the full frequency space is appropriate.

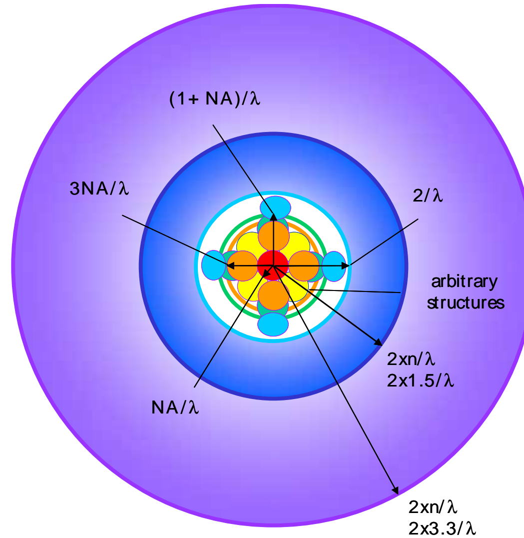

Fig. 5. Available frequency space coverage for various optical systems.

The resolvable dimensions for typical source wavelengths are shown in the Table I. The columns labeled by n_{max} reflect the largest index transparent material of which we are aware at each wavelength. Interestingly, the usual improvement in resolution with wavelength is modified by the transparency regions of high-index materials. Additional materials may further expand the available resolution. At a 193-nm wavelength, the resolution approaches typical SEM resolutions without requiring vacuum and indeed being fully compatible with water immersion. These resolutions are well beyond the current established perceptions of microscopy capabilities and suggest that advances in optical microscopy will have important impacts across a broad swath of science and technology.

Table 1. Resolution limits (grating half-pitch) for various optical configurations at widely available laser wavelengths. (all dimensions in nm).

λ	IIM (air; λ/4)	½-immersion (λ/2(*n*+1); *n* = 1.5)	full immersion (λ/4*n*; *n* = 1.5)	½–immersion (n_{max})	full immersion (n_{max})
1064	266	213	177	116	74 (*n* = 3.6; Si)
633	158	127	106	74	48 (*n* = 3.3; GaP)
488	122	98	81	71	50 (*n* = 2.45, GaN)
193	48	39	32	34	27 (*n* = 1.8; polymer)

Acknowledgments

Support for this work was provided by DARPA. The facilities of the NSF-sponsored NNIN node at the University of New Mexico were used to fabricate the test structures.

#102125 - $15.00 USD Received 29 Sep 2008; revised 11 Nov 2008; accepted 14 Nov 2008; published 25 Nov 2008
(C) 2008 OSA